Local Path Planning with Proximity Sensing for Robot Arm Manipulators

Edward Cheung and Vladimir Lumelsky
Yale University, Center for Systems Science
Department of Electrical Engineering
New Haven, Connecticut 06520

Abstract

In this paper, the problem of sensor-based path planning for robot arm manipulators operating among unknown obstacles of arbitrary shape is considered. It has been known that, in principle, algorithms with proven convergence can be designed for planar and simple three-dimensional robot arms operating under such conditions. However, implementation of such algorithms presents a variety of problems related to covering the robot arm with a "sensitive skin", processing data from large arrays of sensors, and designing algorithms for step-by-step motion planning based on limited information. This paper describes our first results of the implementation studies on strategies for robot motion planning in an uncertain environment.

1. Introduction

Ongoing research in robotic motion planning encompasses two major trends. In one approach, also called the Piano Movers' problem, complete information about the robot and its environment is assumed. A priori knowledge about the obstacles is represented by an algebraic description such as a polygonal representation, and typically assumes an unchanging and static environment [7]. One advantage of the model with complete information is in the possibility to observe an optimality criteria, such as minimum energy, or shortest path required to complete the task. An overview of the research in this area can be found in [1].

Another approach to robot motion planning assumes incomplete information about the environment. Such a situation takes place, for example, when the robot has no a priori knowledge about the environment, but is equipped with a proximity sensor that notifies it of impending collision, or proximity to an obstacle. The area to be sensed can be large such as with the use of ultrasonic range sensors [8] or stereo vision [9], or it can be a small local area if proximity sensors are used [4], such as the optical sensors discussed in this paper. Other reported uses of light in proximity sensors include grasping applications [10] where optical sensors are mounted in the robot gripper, and tactile sensors in fiber optic arrays [11].

It has been shown that the problem of moving a 2-degree of freedom two- or three-dimensional manipulator in an environment with unknown obstacles can be reduced to the problem of moving a point automaton on the surface of a 2-dimensional manifold where obstacles become simple closed curves [2]. The algorithms resulting from this approach, called Dynamic Path Planning (DPP), guarantee convergence, and require the arm to "slide" along or follow the contour of the obstacle.

To realize such algorithms, the robot arm manipulator must have an ability to sense the presence of an obstacle by every point of its body and to identify the points of the body that are in (physical or proximal) contact with the obstacle. To develop this capability, a sensitive "skin" is needed that would cover the whole body of the arm. Such skin would be similar, in case of the physical contact, to the skin of humans or animals; in case of the proximal contact, it would form the kind of aura similar to the hairs on the legs of some insects. Realization of such sensing capabilities encompasses a variety of hardware and data processing issues that, to our knowledge, have not been addressed before.

This paper addresses the implementation issues related to the DPP approach, and, specifically, the problem of instrumenting a robot arm with the sensitive skin and interpreting the sensory data generated by the skin, for the purposes of obstacle avoidance.

A scheme is suggested for obstacle following given the response of the proximity sensors on the arm. The considered approach is based on sensory data supplied by infrared proximity sensors that cover the whole body of the robot arm and thus forming the arm's "sensitive skin". The presented results describe the first stage of our project and treat the problem in the context of motion planning for a planar robot arm.

Suppose that the robot body is covered by proximity sensors that sense a nearby obstacle. Assuming that a global path planning algorithm is in place, local strategy is needed to generate, at the current location of the robot, its next step. What is needed is the local tangent to the obstacle, at the point of contact with the robot; here, "contact" refers to the fact of sensing an obstacle at some distance. Once this is known, the robot can move along this local tangent to accomplish contour following. To generate the local tangent, information is needed on which points of the robot body are experiencing the obstruction; this assures that the next move of the robot does not lead to collision and/or loss of contact with the obstacle.

Below, Section 2 addresses the hardware issues, describes briefly available options, and justifies the choice of proximity sensors. Then, Section 3 addresses algorithmic issues of local step planning.

2. The Proximity Sensor

Apart from providing the robot arm with information about an approaching obstacle, the sensor system should also indicate the location on the arm body where the obstruction takes place. This suggests an array of distance sensors. A useful detection range of about five inches is considered to be adequate. The sensor should remain effective under shallow angles between the obstacle and the sensing beam, and should furthermore have no "dead zones" on the arm body: an obstacle must be detected if it is located within the detectable range of the sensors. Otherwise, if the dead zone comes in contact with an obstacle, a collision may take place. A brief survey of sensor options follows.

The first choice to be made is between passive sensors, such as tactile or vision, and active sensors that operate on emitting a form of energy and sensing the reflected signal. For the considered application, passive sensors do not seem to present a viable alternative. For example, tactile sensing of obstacles in practice would amount to numerous collisions, whereas covering the arm body with sensors, each of which would provide a vision capability, is not practical. Thus, a viable choice must be among active sensors.

Two major types of active sensing make use of optical or acoustical radiation. In addition, inductive and capacitive methods can be used to accomplish sensing, but these methods are generally limited to detection distances of less than one inch, and are dependent on the material of the obstacle. Commercial inductive and capacitive sensors are mainly used in industrial environments where the applications require durability and involve objects of known composition that have to be sensed at very close range.

With acoustic sensing, a burst of ultrasonic energy is transmitted, reflected from an obstacle and then received, making use of the time of flight for distance measurement [5]. A drawback of this type of sensor is that, because the wavelength of sound is relatively long, some obstacles can exhibit specular (mirror like) reflection. Consequently, large flat surfaces may be undetected by the sensor because of the lack of reflected signal. This effect is especially pronounced at shallow angles between the energy beam and the obstacle - a case very common in the considered application.

In addition, commonly available acoustical sensors, such as the popular Polaroid sensor, operate poorly when obstacles are placed closer than 0.9 feet from the sensor [5,8], unless methods such as active damping of the transducer are used [6]. This dead zone necessitates the path planner to restrict the distances of obstacle detection to larger than 0.9 feet from the sensor, which is not realistic in the case of motion planning for arm

manipulators. For example, it may render the target position unreachable if it can be reached only by passing between two obstacles located at about two feet from each other.

To overcome some of these shortcomings, a radiation of shorter wavelength can be used, such as light. The wavelength of visible light is in the range of hundreds of nanometers, tending obstacles to appear matte, scattering light equally in all directions [3]. If the matte surface to be sensed is illuminated by a narrow beam of light, the amount of reflected radiation will depend mainly on the distance between the surface and the receiver. This insensitivity to obstacle orientation can be exploited to detect the presence of objects. One drawback of using light for sensing is that objects of dark colour may not be sensed; also, optical mirrors will continue to exhibit specular reflection, possibly resulting in a lack of returning radiation.

Based on these considerations, a sensor system was chosen based on infrared proximity sensors. The transmitted light is infrared (IR), at a wavelength of approximately 875 nm. This light is modulated at a frequency of 10 kHz, and is then coherently detected after reception to improve immunity to other light sources, such as room lighting. The reflected light is demodulated by a phase locked loop, amplified, and then passed to a digitizer. In the current design, sixteen sensor pairs each consisting of a transmitter and receiver are time multiplexed together, forming one sensor module. The module is manufactured so that all optical components and instrumentation are on one printed circuit board. A sketch of the module appears in Figure 1, and a photograph of a part of the actual module is given in Figure 3; note two sensor pairs highlighted by the reflection in the middle of the black acrylic. The entire sensor system is comprised of a number of these sensor modules mounted on the arm, Figure 4.

In the developed sensor system, the amplitude of the reflected light is used for proximity measurement. An alternative approach, often used in auto focus cameras, is to emit a beam of light and use triangulation to determine distance. The advantage gained by the triangulation method is that the object colour has a reduced effect on the measured distance; on the other hand, optical mirrors continue to be difficult to detect.

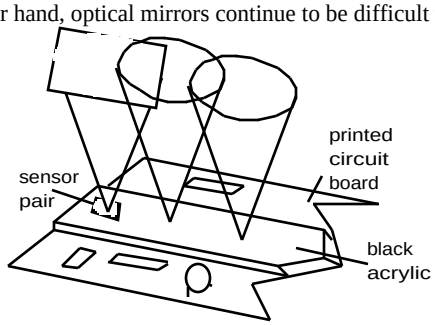

Figure 1. A sketch of the sensor module.

A typical sensor response is shown in Figure 2. The sensor sensitivity becomes insufficient beyond a distance of five inches. If needed, sensing beyond this distance could be supplemented by an acoustical sensor; increasing the transmitted power presents another option.

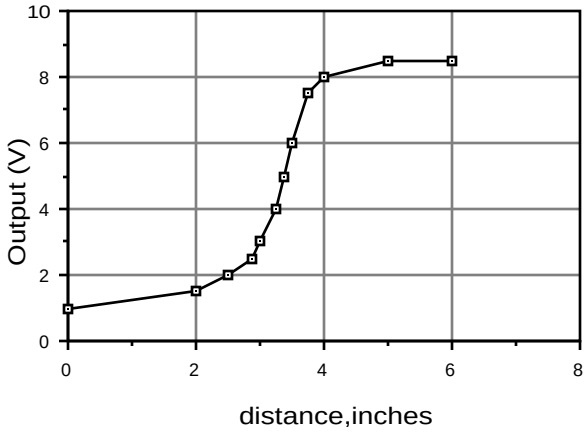

Figure 2. A typical response of the infra-red sensor.

3. Step Planning and Contour Following

In addition to the information about contact with an obstacle provided by the proximity sensor described above, information on the location of the obstacle relative to the arm is also available. It will be shown now how this data is used for contour following. Since the contour following algorithm works in conjunction with the global path planning algorithm [2], the latter is first briefly discussed below.

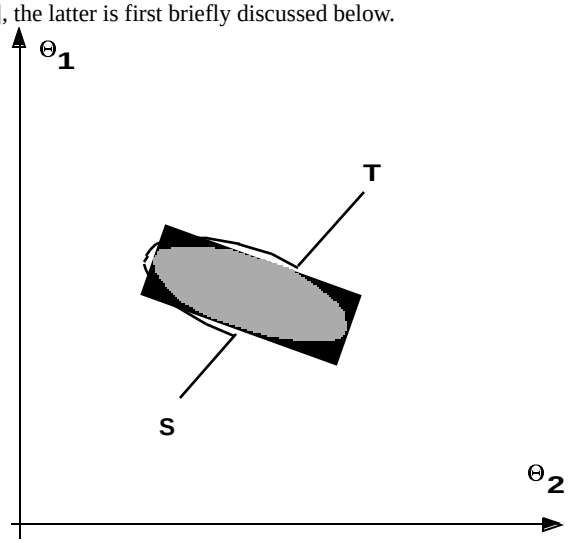

Figure 5. Configuration space of robot arm.

Assume that the robot arm presents a two-link planar structure with two revolute joints Θ_1 and Θ_2, Figure 7. The robot task is to proceed, collision-free, from point S (Start) to point T (Target). Assume for the moment that the robot body is covered with tactile sensors. [Actually, the algorithm can work with any type of proximity sensing]. The robot can be represented by a point automaton in the configuration space (Θ_1, Θ_2), Figure 5. Correspondingly, any obstacle in the work space has its image in the configuration space. In the path planning algorithm, the automaton moves directly to T from its start S along the line segment S - T until an obstacle is encountered. The point of contact is then designated as a hit point. The automaton turns in a prespecified local direction (e.g. left, as in Figure 5) and follows the contour of the obstacle until the line segment S - T is again met at distance from T shorter than the lastly defined hit point. At this point, the automaton follows S - T to T, unless another obstacle is met causing the process to repeat. The algorithm has been shown to converge if the target is reachable, or to conclude in finite time that the target is not reachable if this is the case.

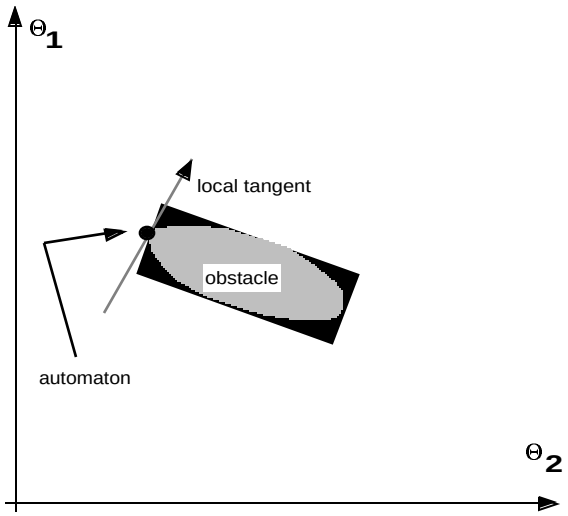

Figure 6. Using the local tangent for contour following.

To realize contour following required by the path planning algorithm, a procedure is needed to plan the next little step along the obstacle boundary at a given location of the robot arm. The input information for the procedure is the current location of the arm and the local tangent to the obstacle boundary, Figure 6. The calculation of the local tangent requires the information on what point(s) of the robot body are in contact with the obstacle in the work space. Note that contour (obstacle) following requires no information about the shape of the obstacle in work space or in configuration space. Below, the procedure for calculating the local tangent is described, followed by the algorithm that uses the local tangent for planning the next step along the obstacle boundary.

Calculation of Local Tangent

The following derivations are valid for a 2 degrees of freedom (dof) revolute - revolute (articulated) arm, Figure 7, but can be similarly derived for other kinematic configurations.

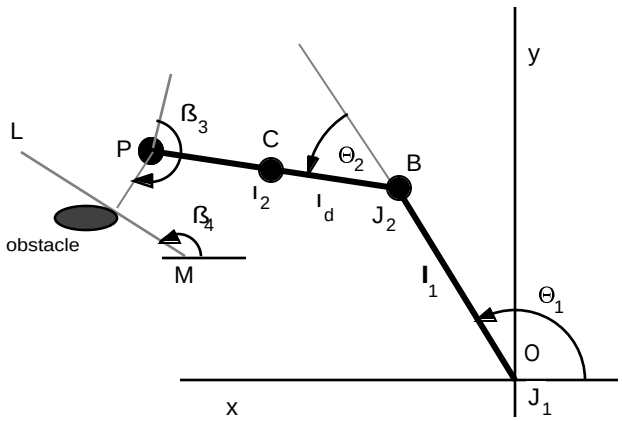

Figure 7. A sketch of the 2-link arm with revolute joints.

In Figure 7, link 1 and link 2 of the arm are represented by the line segments O - B and B - P, of lengths l_1 and l_2, respectively; J_1 and J_2 are arm joints; point P represents the arm wrist; point B, which coincides with joint J_2, represents the arm elbow. Whenever an obstacle is encountered, the arm attempts to slide along its surface. This sliding is accomplished by a coordinated move between joints J_1 and J_2, based on the value of the local tangent LM. To find the latter, estimates of the derivatives $d\Theta_2$ and $d\Theta_1$ are computed at every point along the contour, using the procedure described next.

Depending on their location relative to the arm, obstacles that may occur in the work space are divided into three categories, easily recognizable by the sensor system: type I, type II, and type III, Figure 8. Now we consider each of the types.

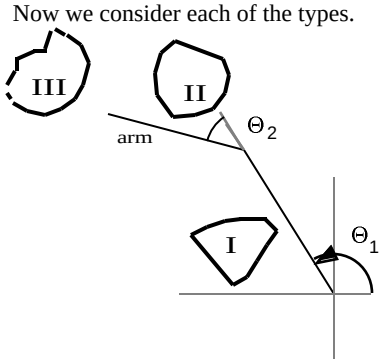

Figure 8. Obstacle types.

Type I are those obstacles that obstruct link 1. It is obvious that since link 2 is irrelevant in such cases, then $d\Theta_1 = 0$ and $d\Theta_2 \neq 0$. Therefore, the local tangent in this case is vertical.

Type II are those obstacles that obstruct link 2. Assume that the arm is obstructed at point C by a type II obstacle, located at link 2 at the distance l_d from the the joint J_2, Figure 7. Then, the estimates of $d\Theta_1$ and $d\Theta_2$ at C can be found as follows. Write the expressions for the x and y coordinates of C, c_x and c_y respectively:

$$c_x = l_1 \cos(\Theta_1) + l_d \cos(\Theta_1+\Theta_2) \qquad (1)$$
$$c_y = l_1 \sin(\Theta_1) + l_d \sin(\Theta_1+\Theta_2)$$

Take total derivatives:

$$dc_x=-l_1\sin(\Theta_1)d\Theta_1+dl_d\cos(\Theta_1+\Theta_2)-l_d\sin(\Theta_1+\Theta_2)d\Theta_1-l_d\sin(\Theta_1+\Theta_2)d\Theta_2$$
$$dc_y=l_1\cos(\Theta_1)d\Theta_1+dl_d\sin(\Theta_1+\Theta_2)+l_d\cos(\Theta_1+\Theta_2)d\Theta_1+l_d\cos(\Theta_1+\Theta_2)d\Theta_2 \qquad (2)$$

Since C is a stationary point, $dc_x=dc_y=0$. Find dl_d from both equations of (2):

$$dl_d = \frac{[-l_1\cos\Theta_1-l_d\cos(\Theta_1+\Theta_2)]d\Theta_1-l_d\cos(\Theta_1+\Theta_2)d\Theta_2}{\sin(\Theta_1+\Theta_2)} \qquad (3)$$

and

$$dl_d = \frac{[l_1\sin\Theta_1+l_d\sin(\Theta_1+\Theta_2)]d\Theta_1+l_d\sin(\Theta_1+\Theta_2)d\Theta_2}{\cos(\Theta_1+\Theta_2)} \qquad (4)$$

Equating the right hand sides and eliminating the denominators in (3) and (4), obtain:

$$\left[\cos(\Theta_1+\Theta_2)\left(-l_1\cos\Theta_1-l_d\cos(\Theta_1+\Theta_2)\right)-\sin(\Theta_1+\Theta_2)\left(l_1\sin\Theta_1+l_d\sin(\Theta_1+\Theta_2)\right)\right]d\Theta_1$$
$$=l_d\left[\cos^2(\Theta_1+\Theta_2)+\sin^2(\Theta_1+\Theta_2)\right]d\Theta_2 \qquad (5)$$

Now, the ratio $d\Theta_2 / d\Theta_1$ is found as

$$\frac{d\Theta_2}{d\Theta_1} = \frac{1}{l_d}\left(-l_1\cos\Theta_1\left(\cos(\Theta_1+\Theta_2)\right)-l_1\sin\Theta_1\left(\sin(\Theta_1+\Theta_2)\right)-l_d\right)$$

$$= -\left(\frac{l_1}{l_d}\left\{\cos\Theta_1\left(\cos(\Theta_1+\Theta_2)\right)+\sin\Theta_1\left(\sin(\Theta_1+\Theta_2)\right)\right\}+1\right) \qquad (6)$$

After simplification, the local tangent to a type II obstacle at point C is given by:

$$\frac{d\Theta_2}{d\Theta_1} = -\left(\frac{l_1}{l_d}\cos\Theta_2 + 1\right) \tag{7}$$

Type III are those obstacles that obstruct the arm wrist or elbow (points P and B, Figure 7). To find the local tangent in this case, the inverse Jacobian of the arm is used [12]. Denote $dx = dP_x$ and $dy = dP_y$ in case the wrist is obstructed, and $dx = dB_x$ and $dy = dB_y$ in case the elbow is obstructed. Then, the following relationship holds:

$$\begin{aligned} d\Theta_1 &= \frac{l_2\cos(\Theta_1+\Theta_2)\,dx + l_2\sin(\Theta_1+\Theta_2)\,dy}{l_1 l_2\cos\Theta_2} \\ d\Theta_2 &= \frac{\left[-l_1\cos\Theta_1 - l_2\cos(\Theta_1+\Theta_2)\right]dx - \left[l_1\cos\Theta_1 - l_2\cos(\Theta_1+\Theta_2)\right]dy}{l_1 l_2\cos\Theta_2} \end{aligned} \tag{8}$$

It is desired that the wrist P slides along the obstacle, which corresponds to moving along the line segment LM, Figure 7. Define $ß_3$ as the angle between the line perpendicular to link 2 and the line from P to the obstacle, and $ß_4$ as the angle between the line LM and the positive x-axis. Then,

$$\frac{dy}{dx} = \tan ß_4$$

$$\text{or} \tag{9}$$

$$dy = dx\,\tan ß_4$$

where $ß_4 = \Theta_1 + \Theta_2 + ß_3$. Substituting the expression for dy from (9) into (8), obtain the ratio $d\Theta_2 / d\Theta_1$:

$$\frac{d\Theta_2}{d\Theta_1} = -\left(\frac{l_1\cos\Theta_1 + l_2\cos\Theta_1\cos\Theta_2 - l_2\sin\Theta_1\sin\Theta_2 + \left[l_1\sin\Theta_1 + l_2(\sin\Theta_1\cos\Theta_2 + \cos\Theta_1\sin\Theta_2)\right]\tan ß_4}{l_2\left[\cos\Theta_1\cos\Theta_2 - \sin\Theta_1\sin\Theta_2 + (\sin\Theta_1\cos\Theta_2 + \cos\Theta_1\sin\Theta_2)\tan ß_4\right]}\right) \tag{10}$$

After simplifying, the expression for the local tangent in the case of a type III obstacle appears as:

$$\frac{d\Theta_2}{d\Theta_1} = -\left(\frac{\frac{l_1}{l_2} + \cos\Theta_2 + \sin\Theta_2\tan(\Theta_2 + ß_3)}{\cos\Theta_2 + \sin\Theta_2\tan(\Theta_2 + ß_3)}\right) \tag{11}$$

Step Planning Algorithm

Every point of contact between the arm body and an obstacle has an associated sensor pair that does the corresponding obstacle detection. For every sensor pair that detects an obstacle, a local tangent is calculated based on the method described above. The motion of the point automaton along a local tangent in configuration space corresponds to the arm "sliding" along the obstacle at the point of contact in the work space. This process is repeatedly done during contour following. Note that one or more obstacles can be sensed simultaneously by more than one sensor pair.

If the chosen local direction is "left", Figure 6, meaning that the robot arm should maneuver around the obstacle in a clockwise fashion, a counterclockwise (ccw) rotation of the calculated local tangent will cause the robot arm to move away from the obstacle, Figure 9. Thus, if the arm is too close to the obstacle, the local tangent can be rotated ccw slightly to increase the distance to the obstacle. The reverse can be done if the sensed obstacle is still at a large distance from the arm. No adjustment is made to the tangent to be followed if the distance to the obstacle is at some preset nominal value. This feedback in the sensor-

based control loop results in constant distance tracking between the arm and the obstacle, thus improving contour following.

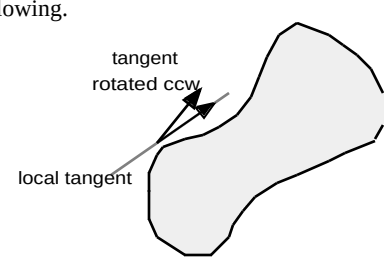

Figure 9. Configuration Space: rotation of local tangent (ccw) causes the robot to move away from the obstacle.

If more than one sensor pair senses one or more obstacles simultaneously, more than one local tangent will be calculated. Then, one of these tangents is selected for planning the next step. The following two examples illustrate this point.

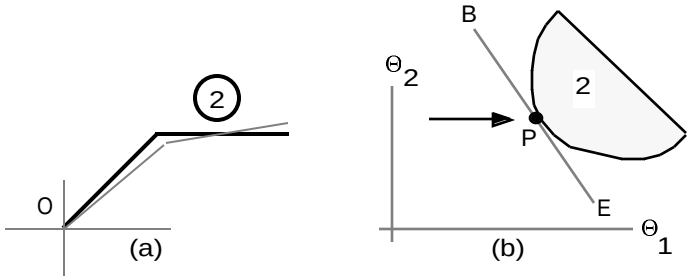

Figure 10. a) Work space, b) configuration space.

Example 1.

Suppose the robot arm is moving towards point P, in the direction of increasing Θ_1, Figure 10b. At this point the arm is obstructed by obstacle 2, which presents an obstacle of type II, Figure 10a. The local tangent at P is EB. In the vicinity of point P, a further increase in Θ_1 will cause collision with the obstacle, Figure 10a. If the local direction is "left", the next move along EB towards point B will cause the arm to slide along obstacle 2 to the position indicated by the dotted line in Figure 10a. Continual recalculation and motion along the resultant tangent constitutes the process of contour following.

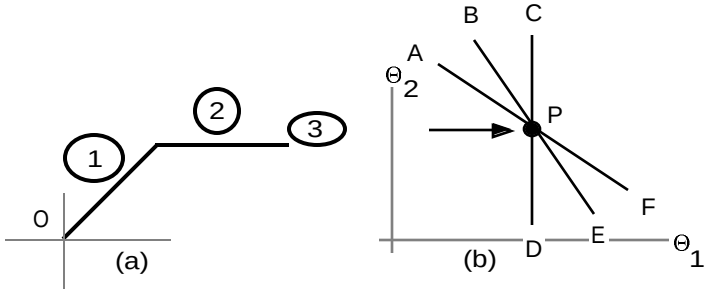

Figure 11. a) Work space, b) configuration space.

Example 2.

For the case with multiple obstructions, suppose the robot arm is moving in the direction of increasing Θ_1, Figure 11b. At point P, the arm is now obstructed by three obstacles that are sensed by the sensor system, Figure 11. A local tangent is then calculated for each obstacle. Obstacles 1,2, and 3, of type I,II, and III, produce tangents CD, BE, and AF respectively. For the local direction "left", the robot can move towards one of the points A,B or C. It is clear from Figure 11 that moving in the direction of point C will cause collision with obstacles 2 and 3. Similarly, moving towards point B will cause collision with obstacle 3. Moving towards point A will cause no collision, and is

therefore the chosen move. The arm moves away from obstacles 1 and 2, and follows obstacle 3's contour. Analogously, a local direction "right" would necessitate a move towards point F for correct contour following.

The system described above has been implemented on a PUMA 560 robot arm, using only the second and third degrees of freedom of this arm. In the present configuration, the real time control system is based on two distributed control boards from Pacific Microcomputers, each of which includes one Motorola 68020 microprocessors, 1 Mbyte of RAM, and Input / Output (I/O) ports. The first board handles the sensor I/O, processing of raw sensor data, and the calculation of local tangent when obstacles are encountered. The second board handles the path planning tasks and I/O functions for the robot servo controls. Combined with the DPP global path planning procedure, the two algorithms described above for step planning and local tangent calculation, proved effective in accomplishing the path planning tasks. In the experiments with various combinations of obstacles, no contact has ever been made with the obstacles, so no collision occurred. No a priori information about the obstacles were given to the robot; path planning was accomplished based only on the on-line information from the sensor system. As anticipated, the required data processing was not significant and fit rather easily into the real-time operation. One of the experimental set-ups, with a C-shaped obstacle, is shown in Figure 4.

References

1. C.K. Yap, Algorithmic Motion Planning. Advances in Robotics, vol. 1: Algorithmic and Geometric Aspects, (J.T. Schwartz and C. Yap, Eds.), Hillsdale, New Jersey: Erlbaum, 1987.
2. V. Lumelsky, Dynamic Path Planning for a Planar Articulated Robot Arm Moving Amidst Unknown Obstacles, Automatica, Sept 1987.
3. D. Ballard, C. Brown, Computer Vision , Prentice-Hall, New Jersey, 1982.
4. M.Winston, Opto Wiskers for a Mobile Robot , Robotics Age, Vol. 3 #1, New Jersey, 1981.
5. Ultrasonic Range Finders, Polaroid Corporation, 1982.
6. G.L.Miller, R.A.Boie, and M.J.Sibilia, Active Damping of Ultrasonic Transducers for Robotic Applications, Proc. IEEE International Conference on Robotics, Atlanta, Georgia, March 1984.
7. J.T. Schwartz and M.Sharir, On the Piano Movers' Problem: I. The Special Case of a Rigid Polygonal Body Moving Amidst Polygonal Barriers, Comm. Pure Appl. Math. 4, 1983.
8. A. Elfes, Sonar-Based Real-World Mapping and Navigation. IEEE Journal of Robotics and Automation, June 1987.
9. L. Matthies and S.A. Shafer, Error Modeling in Stereo Navigation, IEEE Journal of Robotics and Automation, June 1987.
10. D.J. Balek and R.B. Kelly, Using Gripper Mounted Infrared Proximity Sensors for Robot Feedback Control, Proc. 1985 IEEE Conference on Robotics and Automation, St.Louis, Missouri, March 1985.
11. J.S. Schoenwald, A.W. Thiele and D.E. Gjellum, A Novel Fiber Optic Tactile Array Sensor, Proc. 1987 IEEE Conference on Robotics and Robotics and Automation, Raleigh, North Carolina, April 1987.
12. R.P. Paul, Robot Manipulators: Mathematics, Programming, and Control, MIT Press, 1983.

Figure 3. Sensor module.

Figure 4. An experimental set-up with a C-shaped obstacle.